Magma ocean outgassing and hydrogen isotopic constraints on the Hadean Earth

Kaveh Pahlevan[1*], Laura Schaefer[1], Marc M. Hirschmann[2]

1. School of Earth and Space Exploration, Arizona State University, Tempe, AZ, 85287, USA
2. Department of Earth Sciences, University of Minnesota, Minneapolis, MN, 55455, USA

*To whom correspondence should be addressed:

Email: kaveh.pahlevan@asu.edu

Tel: +1 (480) 401 8584

Fax: +1 (480) 965 8102

5 Figures

Submitted to EPSL

Abstract

The Moon-forming giant impact extensively melts and partially vaporizes the silicate Earth and delivers a substantial mass of metal to Earth's core. Subsequent evolution of the terrestrial magma ocean and overlying atmosphere has been described by theoretical models but observable constraints on this epoch have proved elusive. Here, we report calculations of primordial atmospheric evolution during the magma ocean and water ocean epochs and forge new links with observations to gain insight into the behavior of volatiles on the Hadean Earth. As accretion wanes, Earth's magma ocean crystallizes, outgassing the bulk of its volatiles into the primordial atmosphere. The redox state of the magma ocean controls both the chemical composition of the outgassed volatiles and the hydrogen isotopic composition of water oceans that remain after hydrogen escape from the primordial atmosphere. While water condenses and is retained, molecular hydrogen does not condense and can escape, allowing large quantities (~10^2 bars) of hydrogen to be, in principle, lost from Earth in this epoch. Because the escaping inventory of H can be comparable to the hydrogen inventory in primordial water oceans, the corresponding deuterium enrichment can be large with a magnitude that depends on the initial H_2 inventory of the atmosphere. Under equilibrium partitioning, the water molecule concentrates deuterium and, to the extent that hydrogen in other forms (e.g., H_2) are significant species in the outgassed primordial atmosphere of Earth, pronounced D/H enrichments (~2x) in the oceans are expected to arise from equilibrium D/H partitioning alone. By contrast, the common view that terrestrial water has a primarily carbonaceous chondritic source requires seawater to preserve the isotopic composition of that source, undergoing minimal D-enrichment via equilibration with H_2 followed by hydrodynamic escape. Such minimal enrichment places upper limits on the amount of primordial atmospheric H_2 in contact with the early water oceans and implies relatively oxidizing

conditions ($\log fO_2$>IW+1) for last equilibration with the magma ocean. Preservation of an approximate carbonaceous chondrite D/H signature in seawater thus provides evidence that the observed oxidation of silicate Earth occurred before or during the crystallization of the final magma ocean, yielding a new constraint on the timing of this critical event in Earth history. The seawater-carbonaceous chondrite "match" in D/H (to ~10-20%) further constrains the prior existence of an atmospheric H_2 inventory – of any origin – on the post-giant-impact Earth to <20 bars, and suggests that the terrestrial mantle supplied the oxidant for the chemical destruction of metals during terrestrial late accretion.

Keywords: magma ocean; outgassing; water; hydrogen; isotope; Hadean

1. Introduction

The composition and origin of Earth's early atmosphere has been debated since at least the mid-twentieth century (Brown, 1949). Recent interest arises from a desire to understand climate on the early Earth (Wordsworth and Pierrehumbert, 2013a) as well as the environment that led to abiogenesis (Kasting, 2014), and because the volatile history of Earth gives insight into the origin and evolution of the planet more generally. Here, we develop the connection between the history of the fluid envelope and that of the silicate Earth. We use ideas about Earth accretion and insights that they yield for the origin and history of Earth's volatiles. The focus is on Earth's steam atmosphere, a unique reservoir in Earth history that links the energetic process of planetary accretion via giant impact to the emergence of Earth's oceans and Hadean climate. We use "steam atmosphere" to describe any atmosphere prevented from condensation by internal heat in which H_2O is an important component, even those in which other gases (e.g., H_2) are more abundant by number.

A question closely related to the atmospheric composition of the early Earth is the oxygen fugacity (fO_2) of the magma ocean from which the primordial atmosphere was outgassed (Elkins-Tanton, 2008). Plausible fO_2 of magma ocean outgassing range from reducing (H_2-CO-rich) to oxidizing (H_2O-CO_2-rich) atmospheres (Hirschmann, 2012). In analogy with the volatile inventory on modern Earth, prior work has assumed that the primordial atmosphere of early Earth was H_2O-CO_2-rich (Abe and Matsui, 1988; Kasting, 1988). However, given a lack of knowledge about the oxygen fugacity of outgassing, reducing primordial outgassed atmospheres are difficult to rule out (Hirschmann, 2012). Models and measurements of early Earth oxygen fugacity yield contradictory evidence: whereas the fO_2 of metal-silicate equilibration is necessarily reducing ($\log fO_2$<IW-2) due to the co-existence of metals (Wade and Wood, 2005) and implies H_2-CO-rich gas mixtures, the oldest terrestrial samples – Hadean zircons – are characterized by much higher fO_2 consistent with the modern (oxidized) terrestrial mantle, and suggest an H_2O-CO_2-rich atmosphere (Trail et al., 2011). Some process apparently oxidized the silicate Earth during or shortly after core formation (Delano, 2001). Because the nature and timing of this process are as yet unclear, the chemical composition and oxidation state of Earth's early atmosphere remain unknown.

Here, by linking the hydrogen isotopic composition of the terrestrial oceans to the chemical composition of the primordial atmosphere, we articulate new constraints on the oxygen fugacity of magma ocean outgassing and subsequent processes on the Hadean Earth. Because this model is constrained by isotopic observations, it has the potential to yield new insights into early Earth evolution. Several features of early Earth evolution render the D/H composition of the oceans a reflection of the magma ocean and Hadean

atmospheric processes: (1) most of the water gained by Earth during planet formation was already accreted at the time of the Moon-forming giant impact and therefore participated in the terminal terrestrial magma ocean (Greenwood et al., 2018), (2) most (>75-98%) of the water initially dissolved in the magma ocean was outgassed into the atmosphere upon solidification, rendering the terrestrial water oceans the dominant exchangeable water reservoir on early Earth (Elkins-Tanton, 2008), and (3) the residence time of water in the terrestrial oceans with respect to the subduction and the deep water cycle is long, of order ~10^{10} years (van Keken et al., 2011). Together, these observations suggest that most hydrogen atoms currently residing in the oceans experienced the magma ocean and its aftermath and carry isotopic memory from these early epochs. The inference that the modern oceans reflect the isotopic composition of Hadean oceans – and, indeed, the bulk silicate Earth – is supported by measurements on Archean samples with D/H values for seawater identical to modern values to within a few percent (Pope et al., 2012). Percent-level variations in ocean D/H can arise due to exchange of water with the solid Earth due to plate tectonic processes (Kurokawa et al., 2018; Lécuyer et al., 1998) but here we are interested in large magnitude D/H variations (~2x) that can arise due to early atmospheric processes (see §4.3).

The isotopic composition of the oceans is determined by deuterium fractionation between H_2O and H_2 and the contrasting histories of these molecules in the planetary environment. Hydrogen (^1H) and deuterium (^2H) in water and molecular hydrogen experience distinct vibrational frequencies due to different bond strengths associated with the O-H and H-H stretch. These contrasting bonding environments result in deuterium begin concentrated into water molecules while molecular hydrogen is deuterium-depleted at equilibrium, especially at low temperatures, i.e. isotopic fractionation occurs between the water ocean

101 and H_2-rich atmosphere. Hence, even in the absence of HD/H_2 mass fractionation during
102 the escape process (Zahnle et al., 1990), loss of molecular hydrogen from the early Earth
103 can enrich planetary water in deuterium due to low-temperature equilibrium partitioning
104 alone, i.e. light isotopes are concentrated into the escaping gas relative to the oceans.
105 This equilibrium partitioning between molecules can result in isotopic evolution of the
106 terrestrial oceans due to the contrasting fates of molecular hydrogen and water on early
107 Earth. As on the modern Earth, water vapor is expected to be confined to the lower
108 atmosphere via condensation at the tropopause (Wordsworth and Pierrehumbert, 2013b)
109 and retained on the Hadean Earth while hydrogen in non-condensable forms (e.g., H_2)
110 can traverse the tropopause and undergo large-scale escape (Hunten, 1973). To the extent
111 that the isotopic composition of escaping gas was distinct from that of oceans, isotopic
112 evolution would have taken place.
113
114 That the hydrogen isotopic composition of the terrestrial oceans retains memory of early
115 epochs permits its use in constraining early atmospheric fractionation processes, pending
116 knowledge of the D/H of its source. Indeed, the source of the Earth's hydrosphere is
117 commonly inferred from the D/H composition of the oceans in comparison with Solar
118 System sources such as comets, asteroids (via meteorites), and the solar nebula (via
119 Jupiter). Based on hydrogen and nitrogen isotopic evidence, the major terrestrial volatiles
120 (C, N, H) are commonly inferred to be sourced primarily from carbonaceous chondrites
121 (Alexander et al., 2012; Halliday, 2013; Marty, 2012). The close "match" (to within
122 ~10%) between seawater D/H and the carbonaceous chondrite distribution peak – if not
123 genetic – must be relegated to coincidence with a priori low probability (Lécuyer et al.,
124 1998). Although a predominantly nebular source for terrestrial hydrogen with strong D/H
125 fractionation has been explored (Genda and Ikoma, 2008), the nitrogen isotopic

126 evidence, in particular, argues against a predominantly nebular source for Earth's
127 volatiles (Alexander et al., 2012; Marty, 2012). We adopt the common view that
128 terrestrial seawater has a primarily carbonaceous chondritic source and show that the
129 preservation of such a chondritic D/H signature in the terrestrial oceans places an upper
130 limit on H_2 abundances on the Hadean Earth, requires oxidizing conditions for magma
131 ocean outgassing ($H_2/H_2O<0.3$), and suggests a limited role for H_2 production via the
132 iron-water reaction during terrestrial late accretion.
133
134 The outline of the paper is as follows. In §2, we estimate equilibration timescales between
135 the magma ocean and primordial atmosphere and present calculations that relate the
136 chemical composition of the outgassed atmosphere to the oxidation state of the magma
137 ocean. In §3, we describe a climate model that considers greenhouse warming by the
138 primordial H_2 inventory in the subsequent water ocean epoch and the timescales that
139 govern its evolution. In §4, we describe the results of the model for the hydrogen isotopic
140 evolution of the oceans due to equilibration and loss of a primordial H_2 inventory. In §5,
141 we discuss the implications of these results for the oxidation state of the magma ocean
142 and the oxidant for terrestrial late accretion, and in §6, we summarize and conclude. The
143 envisioned sequence explored in this paper is summarized in Figure 1.

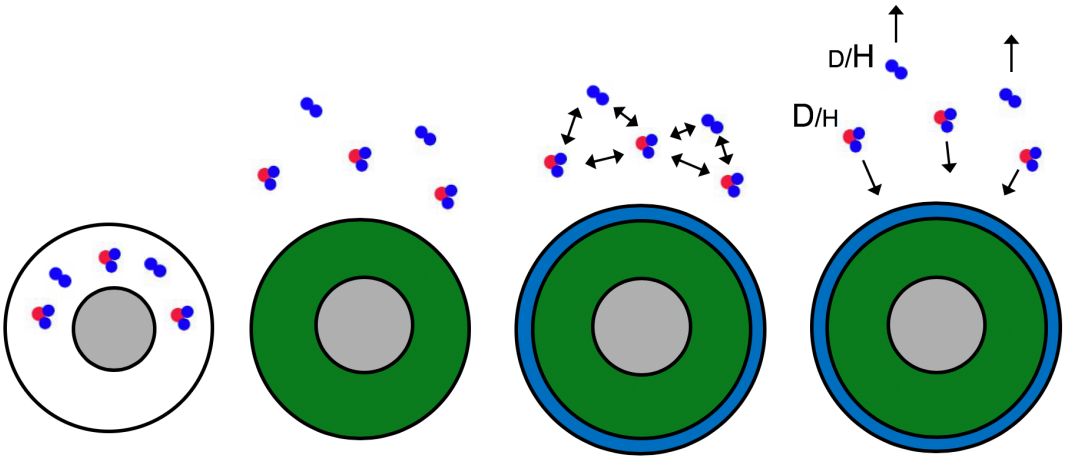

Figure 1 – Behavior of hydrogen on Earth after the Moon-forming giant impact. (a) After the giant impact, a deep magma ocean dissolves most of the hydrogen accreted to Earth, (b) crystallization of the magma ocean leads to primordial outgassing of most of exchangeable hydrogen with H_2/H_2O determined by oxygen fugacity of last equilibration with the magma ocean (§2.2), (c) condensation of the oceans and low-temperature (~300-500K) H_2O-H_2 D/H equilibration leads to deuterium-enrichments (H_2O) and depletions (H_2) in co-existing species, (d) retention of water via condensation coupled with loss to space of deuterium-depleted H_2 via hydrodynamic escape leads to deuterium enrichment in the terrestrial oceans whose magnitude depends on the initial H_2/H_2O of the outgassed atmosphere.

2. Magma ocean outgassing

Magma oceans may arise in the early Solar System through various processes (Elkins-Tanton, 2012). The Moon-forming giant impact extensively melts the silicate Earth and leaves the accreting planet with ~99% of its final mass (Pahlevan and Morbidelli, 2015). During the ensuing magma ocean crystallization period, terrestrial water transitions from being predominantly dissolved in the magma ocean to primarily outgassed into the steam atmosphere, subsequent condensation of which forms the early terrestrial oceans (Elkins-

151 Tanton, 2008). This event is therefore considered the major volatile processing event in
152 early Earth history, after which the abundance and initial distribution of terrestrial water
153 is largely established and planetary processes transition from the accretionary to the
154 geological regime. In this section, we first justify the use of equilibrium thermodynamics
155 in calculating atmospheric compositions (§2.1) and then discuss the dependence of the
156 outgassed gaseous composition on the redox state of the magma ocean at the time of last
157 equilibration with the atmosphere (§2.2).
158
159 2.1. Magma ocean-atmosphere equilibration timescales
160 To justify the use of equilibrium thermodynamics, we first examine equilibration times
161 between the magma ocean and the overlying atmosphere. On the modern Earth, the
162 timescale for pCO_2 equilibration with the oceans is ~10^2 years (Archer et al., 2009), but
163 no equivalent empirical estimate exists for magma ocean-atmosphere equilibration.
164 Using a boundary-layer analysis (Hamano et al., 2013), we estimate the timescale for
165 magma ocean-atmosphere equilibration assuming that diffusion through the magma
166 surface boundary layer, rather than ascent of bubble plumes, dominates the equilibration
167 process. We consider a schematic sequence in which thermal boundary layers form at
168 the magma ocean surface and are peeled away by negative buoyancy. The equilibration
169 timescale can then be estimated:

170 $$\tau_{eq} = \tau_{BL} x N = (\delta_T^2/\kappa) x (z/\delta_C) \quad (1)$$

171 where τ_{BL} is the timescale for the formation of a thermal boundary layer, and N is the
172 number of formation and buoyant destruction cycles before the entire magma ocean mass
173 is processed through the surface boundary layer, δ_T and δ_C are the thermal and chemical
174 boundary layer thicknesses, respectively, κ is the thermal diffusivity of the magma (cm^2

175 s^{-1}), and z is magma ocean depth. We can express the thickness of the chemical boundary
176 layer in terms of the thickness of the thermal boundary layer via scaling: $(\delta_C/\delta_T) =$
177 $(D/\kappa)^{1/2}$ where we take D as the atomic diffusivity for water in magma (cm^2 s^{-1}). For
178 parameter choices, we adopt a thermal diffusivity (κ=2x10^{-3} cm^2 s^{-1}) appropriate to
179 peridotite liquid (Lesher and Spera, 2015) and an atomic diffusivity for water in magma
180 (D_w=1.4x10^{-4} cm^2 s^{-1}) appropriate for a basaltic magma with ~1 wt% water at 2000 K
181 (Zhang et al., 2007). Substitution of these parameters yields an estimate for equilibration
182 timescales:

183 $$\tau_{eq} = 3x10^3 years\ x\ \left(\frac{\delta_T}{1cm}\right) x \left(\frac{z}{500\ km}\right) \quad (2)$$

184 This result suggests that equilibration with the atmosphere by processing the magma
185 ocean through a chemical boundary layer is rapid relative to cooling timescales, which
186 are estimated at ~10^6 years (Lebrun et al., 2013). Although more work is required to
187 quantify the competing role of magma outgassing via bubble plumes in accommodating
188 the super-saturation near the surface (Ikoma et al., 2018), this treatment suggests that
189 equilibration via boundary layer diffusion alone may be sufficiently rapid to motivate the
190 equilibrium assumption.
191
192 2.2. Primordial atmospheric compositions
193 A fundamental parameter governing equilibrium compositions of outgassed atmospheres
194 is the oxygen fugacity (fO_2). As long as the redox buffering capacity of the magma ocean
195 exceeds that of the outgassed atmosphere, the magma ocean determines the fO_2 of the
196 atmosphere with which it equilibrates (Hirschmann, 2012). Volatile outgassing from the
197 magma ocean continues until the end of magma ocean crystallization, when the
198 formation of a meters-thick solid chill crust effectively isolates the newly formed

atmosphere from exchange with silicate Earth. Therefore, the initial composition of the atmosphere during the Hadean is dictated by last equilibration with the magma ocean.

Despite its importance to planetary evolution, the fO_2 at the magma ocean-atmosphere interface is not well-constrained. There are two end-members: (1) in analogy with the modern Earth mantle, the magma ocean-steam atmosphere system may be chemically oxidized ($\log fO_2$~QFM), with water vapor and carbon dioxide dominant (Abe and Matsui, 1988; Kasting, 1988). However, (2) the terrestrial magma ocean – having held metallic droplets in suspension – may also be much more reducing ($\log fO_2$~IW-2) at the surface where equilibration with the atmosphere takes place. Under such reducing conditions, H_2 and CO are the dominant H- and C-bearing gaseous species (Fig. 2). A remarkable feature of magma oceans is that the expected range of possible fO_2 values spans the transition from the reducing (H_2-CO-rich) to oxidizing (H_2O-CO_2-rich) gas mixtures, indicating a rich volatile-processing history during planetary accretion.

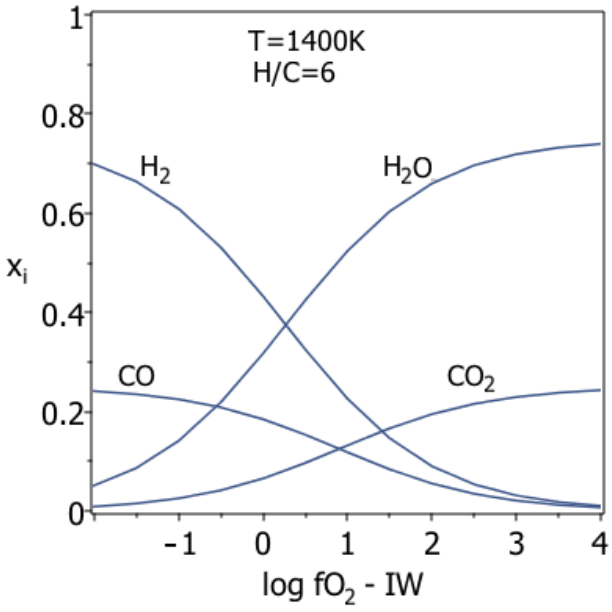

Figure 2 – High-temperature equilibrium outgassed atmospheres. The mole fraction of vapor species is calculated as a function of oxygen fugacity (fO_2) relative to the iron-wüstite (IW) buffer at an equilibrium temperature of 1,400 K. Parameters for the IW buffer are given in (Frost, 1991). Thermodynamic data for gaseous species (H_2O-H_2-CO-CO_2) are adopted from (Chase et al., 1985). The lower end of the range of logfO_2 (IW-2) characterizes oxygen fugacity of a magma ocean in equilibrium with a suspension of metallic droplets, whereas the upper end of the range (IW+4≈QFM) corresponds to the redox state of oxidized modern Earth mantle.

213 Calculation of climate (§3) requires specification of the mass and molecular composition
214 of the atmosphere. Whereas an oxidizing (H_2O-CO_2-rich) outgassed gaseous envelope
215 experiences minimal chemistry upon cooling and maintains its molecular composition,
216 evolution of a reducing (H_2-CO-rich) gaseous envelope may involve more significant
217 transformations. As the envelope cools following magma ocean crystallization, the

reaction ($3H_2+CO \Leftrightarrow CH_4+H_2O$) shifts to the right, potentially converting the outgassed gas mixture into a methane-rich atmosphere before quenching and condensation of the oceans (Schaefer and Fegley, 2010). Nevertheless, we consider CH_4 to be – at most – a transient molecule in the primordial atmosphere because it is unstable with respect to UV photolysis via Lyman α emission. The photolysis of methane under the influence of the UV flux of the young Sun occurs rapidly, at a rate of ~1 bar/Myrs (Kasting, 2014), with the carbon oxidized to CO/CO_2 and the hydrogen reverting to molecular form before escaping, analogous to the modern atmosphere of Titan. The photochemical stability of H_2 suggests that the reducing power inherited from the magma ocean is primarily carried by, and lost via the escape of, molecular hydrogen.

3. Climate model

In this section, we describe a climate model used to calculate surface temperatures due to H_2 greenhouse warming, which we use in the next section (§4) to determine the relative behavior of hydrogen and deuterium on the Hadean Earth. Following magma ocean crystallization, H_2O in the outgassed atmosphere becomes the early oceans. The partial pressure of H_2O is then determined by vapor pressure equilibrium at surface temperatures determined by solar radiative balance. Hence, soon after magma ocean crystallization, the Hadean Earth will relax into a solar-powered climate with early water oceans co-existing with a massive non-condensible primordial atmosphere. While oxidizing (H_2O-CO_2-rich) ocean climates have previously been described (Wordsworth and Pierrehumbert, 2013b), equivalent reducing (H_2O-H_2-rich) ocean climates have not. To describe the evolution of the earliest Hadean climate, we adopt a 2-component (H_2O-H_2) chemical model for the atmosphere and ocean and take the oxygen fugacity of last equilibration between the magma ocean and primordial atmosphere (and hence outgassed

243 H_2/H_2O) as a free parameter. Because water condenses in the lower atmosphere and is
244 retained but molecular hydrogen can escape, the free parameter governing early climate
245 can be expressed as the inventory of molecular hydrogen in the atmosphere (pH_2).
246
247 Due to water condensation and cold-trapping in the lower atmosphere and collision-
248 induced infrared opacity of H_2 at high (>0.1 bar) pressures, the emission level in H_2O-
249 H_2 model atmospheres is determined by the opacity of H_2 (Wordsworth, 2012). The
250 emission temperature (T_E) is given by top-of-the-atmosphere radiative balance with the
251 early Sun:
252 $$\frac{L}{4}(1-A) = \sigma_{SB} T_E^4 \quad (3)$$
253 with L the solar constant, A the visible bond albedo, and σ_{SB} the Stefan-Boltzmann
254 constant. For $L=10^3$ W/m^2 appropriate for the early Sun and a bond albedo A=0.3, an
255 emission temperature of 235 K is obtained for the primordial Earth. For simplicity, solar
256 luminosity in these calculations is held constant. Results are qualitatively similar for a
257 range of emission temperatures (215-255 K), as might be expected based on an evolving
258 Sun, cloud feedback and/or by adjusting the planetary albedo to account for increased
259 Rayleigh scattering in thicker atmospheres. These effects are known to alter the radiation
260 budget by tens of percent (Gough, 1981; Wordsworth, 2012). At infrared wavelengths,
261 the optical depth unity surface of a pure H_2 atmosphere has been calculated for a several
262 Earth-mass planet (g=20 m/s^2, T_{ph}=100 K) and is ~0.2 bars (Wordsworth, 2012).
263 Combining the expressions for photospheric pressure ($P_{ph} \propto g/\kappa$) and collision-induced
264 opacity ($\kappa \propto \rho$) of an ideal gas ($\rho \propto P_{ph}/T_{ph}$) yields a scaling relation for photospheric
265 pressure, gravitational acceleration, and photospheric temperature ($P_{ph} \propto g^{1/2} T_{ph}^{1/2}$).
266 Applying this scaling relation to the emission temperatures (T_{ph}=235K) relevant to the
267 Hadean Earth (g=9.8m/s^2) yields an H_2 photospheric pressure ~0.21 bars, which we

adopt. Since the atmosphere at the emission level is cold and dry, this pressure – appropriate for a pure H_2 atmosphere – is taken as the emission pressure to which a moist adiabatic structure (see below) must be stitched.

Planetary surface temperature is controlled by the structure of the troposphere. At the base of the troposphere, vapor pressure equilibrium with the ocean controls the water vapor abundance. We assume a troposphere saturated in water vapor throughout. Accordingly, the partial pressure of water vapor is given by $p_{H2O} = \exp(-\Delta G/RT)$, with $\Delta G=\Delta H-T\Delta S$ and $\Delta H=40.58$ kJ/mol, $\Delta S=0.1082$ kJ/mol.K (Chase et al., 1985). As in any multi-component atmosphere, the inventory of one gas influences the partial pressure of other gases through vertical redistribution (Wordsworth and Pierrehumbert, 2013a). The total pressure is assumed given by the expression $p_T = \sigma_{H2O} g\mu/\mu_{H2O} x_{H2O}$ with σ_{H2O} the surface density of water vapor, g the gravitational acceleration at the surface, μ the mean molecular weight, and μ_{H2O} and x_{H2O} the atomic mass and the mole fraction of water vapor. This expression is strictly valid in a well-mixed atmosphere, which we take as an adequate approximation for an H_2O-H_2 atmosphere. With the above relations, we write an expression for the entropy of atmospheric gas in contact with the oceans, which we use to calculate surface temperature. The entropy of the troposphere is that of the basal gaseous mixture:

$$S(T) = \sum_i x_i s_i(\mathrm{T}) - \mathrm{R}\sum_i x_i \ln x_i - \mathrm{R}\ln\mathrm{P} \quad (4)$$

which is the expression for entropy of an ideal mixture of ideal gases, with the first term the sum over species as pure gases at standard pressure, the second term an entropy of mixing term deriving from the fact that the gas parcel is a mixture of randomly distributed gas molecules, and the third term a pressure correction due to the volume available to each molecule. In this way, the entropy of the atmospheric parcel at any temperature (T),

pressure (P) and composition (x_i) can be calculated. We consider ideal gas theory as an adequate approximation for the primordial atmosphere because intermolecular distances are large relative to the size of the molecules. The thermodynamic data for the entropy of pure substances is also taken from standard sources (Chase et al., 1985).

Since a moist adiabat is also isentropic, the tropospheric entropy can be used to relate the conditions at the base to those characterizing the radiative emission level where the mode of energy transport transitions to radiation. A major influence on tropospheric structure is the condensation of water vapor into clouds through adiabatic expansion and cooling. The specific entropy at the radiative emission level at the top of the troposphere must therefore consider condensates:

$$S(T) = F_v S_v(\mathrm{T}) + F_L S_L(\mathrm{T}) \quad (5)$$

with F_V and F_L the fraction of total molecules in the parcel in the gas and condensates, respectively. Atmospheric P-T paths determined by calculating pseudoadiabats (i.e., with rainout) are similar to adiabatic equivalents (i.e. with suspended condensates) (Ingersoll, 1969), permitting use of a two-phase isentrope even when rainout might be expected and upper tropospheric opacity determined by gas-phase (H_2) opacity alone. The procedure for calculating surface temperature then entails: (1) an initial estimate for the surface temperature, yielding the partial vapor pressure of water vapor and, with a given H_2 inventory, the total atmospheric surface pressure, (2) calculation of the entropy of the convective atmosphere, (3) evaluation of thermodynamic state, including temperature, of the atmospheric parcel at a pressure of 0.21 bars representing the radiative emission level. In this way, each value of surface temperature corresponds to a value of emission temperature, and iteration allows identification of the surface temperature corresponding to the emission temperature required by top-of-the-atmosphere radiative balance

318 (Equation 3). Because the convective troposphere is isentropic, we can solve for the
319 surface temperature as a function of emission temperature without explicitly resolving
320 the vertical structure in the intervening atmosphere. In this way, we calculate surface
321 temperatures in the all-troposphere approximation (Pierrehumbert, 2010) and iterate to
322 find solutions.
323
324 **4. Results**
325 In this section, we describe the results of the climate model (§4.1) and use the results to
326 compare the timescales for ocean-atmosphere isotopic equilibration with atmospheric
327 escape (§4.2) to motivate equilibrium isotopic partitioning to describe the behavior of
328 hydrogen and deuterium on the early Earth. Finally, we discuss the hydrogen isotopic
329 evolution of the Hadean oceans and the derived upper limit on pH_2 on the early Earth
330 (§4.3).
331
332 4.1. Equilibrium average surface temperatures
333 Greenhouse warming by ~1-10^2 bars of equivalent H_2 on the Hadean Earth yields surface
334 temperatures ~300-550 K (Fig. 3). Despite some uncertainty arising from cloud feedback
335 or higher albedo due to greater Rayleigh scattering, multi-bar atmospheric H_2 inventories
336 are sufficient to keep Earth out of a snowball state via H_2 opacity alone. The calculation
337 assumes radiative transfer in the terrestrial planet regime, where a sufficient fraction of
338 the visible flux penetrates the atmosphere and powers convection throughout the
339 troposphere, whereas for pH_2>20 bars visible photons might not penetrate, creating a
340 deep atmospheric structure governed by geothermal rather than solar heating as in
341 interior of the giant planets (Wordsworth, 2012). Calculated surface temperatures for
342 pH_2>20 bars are therefore upper limits. These calculations suggest that the dominant

343 control on the surface temperatures in the Hadean is the atmospheric H_2 inventory and
344 that the earliest climate on Earth was warm and governed by the physics of atmospheric
345 escape.

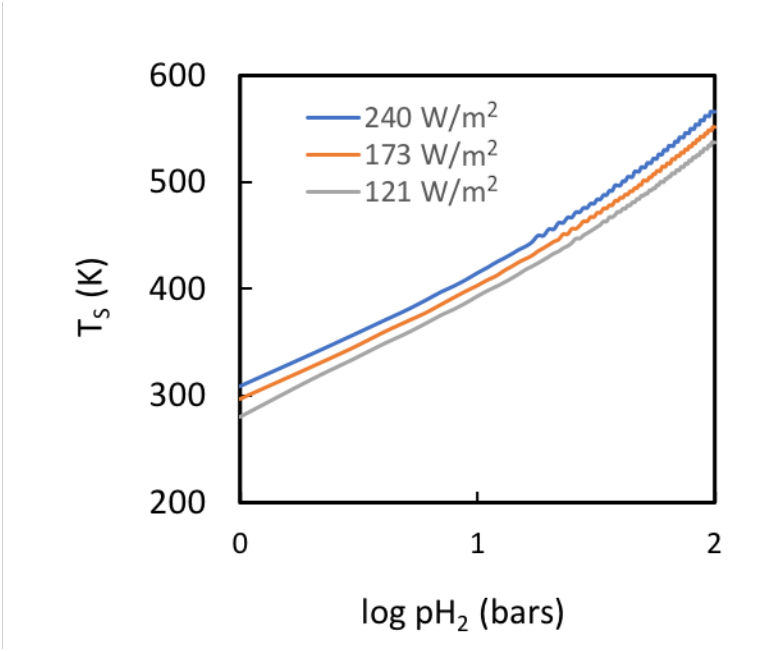

Figure 3 – Ocean surface temperature as a function of primordial H_2 inventory. Temperatures are shown for different values of the outgoing longwave radiation (OLR) flux for emission temperatures of 215, 235, and 255 K, corresponding to a range (0-0.5) of planetary bond albedos. The primordial planetary climate depends primarily on the H_2 inventory. The dominant control on earliest climate in these scenarios is the physics of atmospheric escape.

346 4.2. Atmospheric equilibration and escape timescales

347 Surface temperatures derived from the climate model can be used to assess H isotopic
348 equilibration between the oceans and the atmosphere. A key comparison is between the
349 equilibration time and the residence time of atmospheric H_2. H_2O-H_2 isotopic exchange
350 may be rate-limited by exchange in the atmosphere, because H_2 dissolves negligibly in

the water oceans. Isotope exchange between water vapor and molecular hydrogen is rapid and highly temperature-dependent (Lécluse and Robert, 1994). After the condensation of the steam into water oceans (§3), a significant H_2 inventory (>10-100 bars H_2) and high surface temperatures (>400-550 K, Fig. 3) result in extremely rapid atmospheric reactions such that the timescale for ocean-atmosphere equilibration is limited by the rate of ocean evaporation and circulation of water through the atmosphere in a hydrological cycle. This timescale (≡depth of oceans/evaporation rate) is rapid (≈10^3 years), and nominally independent of H_2 inventory and surface temperature (e.g. pH_2>3 bars, Fig. 4). Ocean-atmosphere isotopic equilibration during the Hadean is therefore expected to initially proceed rapidly. As the primordial climate evolves due to H_2 escape, reaction rates decline until ocean-atmosphere equilibration becomes rate-limited by exchange reactions in the atmosphere. In this regime, the equilibration time between the oceans and atmosphere is given by:

$$\tau_{AO} = (\tau_{ex}/\tau_{res}) x\, \tau_{cir} \quad (6)$$

with τ_{ex} the isotopic exchange time between atmospheric H_2 and H_2O, τ_{res} the residence time of atmospheric water vapor, and τ_{cir} the timescale to circulate the entire oceans through the atmosphere via evaporation and precipitation in a global hydrological cycle (Genda and Ikoma, 2008). As the atmospheric H_2 inventory is lost, the ocean-atmosphere equilibration time evolves for two reasons: (1) the isotopic exchange timescale (τ_{ex}) increases due to the cooling temperatures, (2) the residence time of water vapor in the atmosphere (=depth of equivalent water layer/precipitation rate) decreases due to the lower water vapor pressures associated with lower temperature. Both effects prolong the equilibration time between the ocean and atmosphere, which increases rapidly at low temperatures (pH_2<3 bars, Fig. 4), approaching ~1 Myrs for H_2 inventories of ~1 bar.

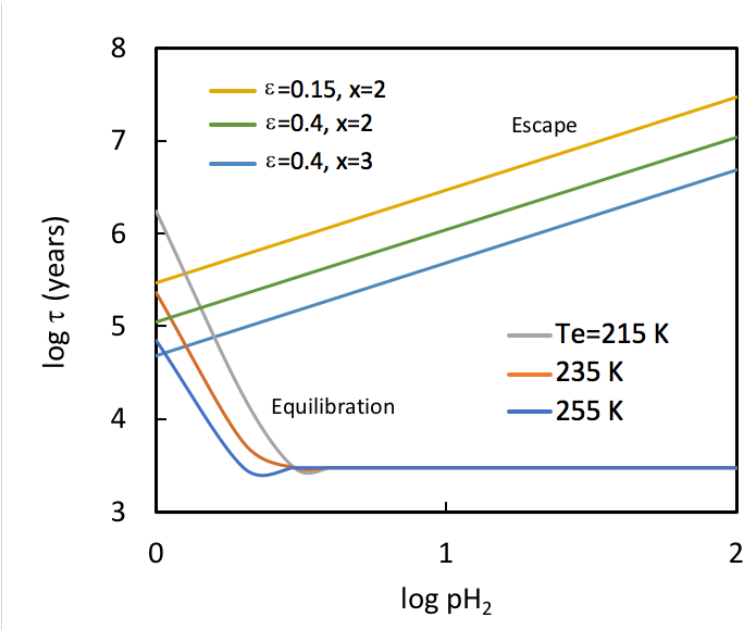

Figure 4 – Ocean-atmosphere isotopic equilibration and hydrodynamic escape versus primordial H_2 inventories. Isotopic equilibration between the water oceans and a primordial H_2-rich atmosphere is calculated for three values of the top-of-the-atmosphere emission temperature (T_e), as a function of total atmospheric H_2 inventory. At high H_2 inventories (e.g. 10-100 bars equivalent H_2), the equilibrium temperatures are high (~400-500K, Fig. 3), and isotopic exchange reactions are extremely fast. Parameters characterizing the escape times are the thermal efficiency (ε) and planetary EUV absorption radii (x) (§4.2). Timescales for ocean-atmosphere equilibration are generally shorter than the residence time of atmospheric H_2 with respect to escape suggesting continuous equilibration during the escape process.

Ocean-atmosphere isotopic equilibration requires that the equilibration time be shorter than the residence time of H_2 in the atmosphere. To determine whether or not this is the case, we calculate extreme ultraviolet (EUV) powered escape rates (Watson et al., 1981) for initial H_2 inventories, and adopt the assumption that loss to space is the sole H_2 sink,

379 as expected on the prebiotic Earth. Escape rates can be calculated using the energy-
380 limited approximation:

381 $$\phi_{H_2} = \frac{\epsilon F_{EUV}}{4R_p} x^2 \qquad (\text{Pa s}^{-1}) \qquad (7)$$

382 with ϕ the hydrogen escape flux expressed as atmospheric pressure loss per unit time,
383 F_{EUV} the extreme ultraviolet flux of the young sun, ε the thermal efficiency or the fraction
384 of incident EUV used to power the planetary wind (ε=0.15-0.4), R_p the planetary radius,
385 and x($\equiv R_{EUV}/R_p$) the effective EUV absorption radius in planetary radii (x=2-3), which
386 characterizes the distended nature of EUV absorption in escaping atmospheres. F_{EUV} is
387 assumed equal to 100x the modern extreme ultraviolet flux, i.e. 464 erg cm^{-2} s^{-1} (Ribas
388 et al., 2005). Other parameter choices (ε,x) are adopted from hydrodynamic calculations
389 of hydrogen-rich atmospheres exposed to comparable EUV fluxes (Erkaev et al., 2016).
390 Calculated H_2 residence times ($=pH_2/\phi_{H2}$) are $\approx 10^6$-10^7 years for atmospheric inventories
391 ≈ 10-100 bars (Fig. 4). Timescales for ocean-atmosphere equilibration are generally
392 shorter than residence times of H_2 in the atmosphere, suggesting continuous equilibration
393 with ocean-atmosphere quenching occurring at H_2 inventories of only ~a few bars.
394
395 4.3. Hydrogen isotopic evolution of the Hadean oceans
396 Finally, we quantify the behavior of hydrogen (^1H) and deuterium (^2H) as tracers of early
397 Earth evolution to articulate constraints on the chemical composition of the primordial
398 atmosphere. In brief, water vapor is retained via condensation but hydrogen in non-
399 condensable form (e.g. H_2) interacts with water vapor in the lower atmosphere and is
400 transported to the upper atmosphere and lost to space. Equilibrium D/H partitioning
401 between water and hydrogen is calculated from standard prescriptions (Richet et al.,

1977).[1] While this prescription strictly relates water vapor to molecular hydrogen, it can also be used to characterize equilibrium between water oceans and H_2-rich atmospheres because the vapor pressure isotope effect relating liquid water to water vapor is an order of magnitude smaller and can therefore be neglected to first order. H_2O-H_2 equilibration is among the largest equilibrium fractionations between two molecules in nature, with a clearly resolvable magnitude at planetary temperatures. D/H composition of planetary oceans therefore reflects the mass of early H_2 reservoirs and the temperatures of isotopic equilibration. To the extent that atmospheric H_2 reservoirs comparable to the terrestrial oceans were present, the D/H composition of the hydrosphere could have evolved dramatically due to equilibrium partitioning and removal of the isotopically light H_2.

The hydrogen isotopic evolution of Hadean oceans can be calculated using equilibrium ocean-atmosphere partitioning. Following magma ocean crystallization, most of the water vapor condenses into oceans, while most H_2 partitions into the atmosphere, generating the earliest climate via radiative balance with the Sun (§3). The magnitude of greenhouse warming for a freshly outgassed atmosphere is significant: only a few percent of the outgassed volatile inventory need be in the form of molecular hydrogen to prevent a snowball Earth and to stabilize a water ocean climate via H_2 greenhouse warming alone (Fig. 3). The existence of such an early greenhouse climate permits isotopic equilibration between the ocean and atmosphere (§4.2) with the temperature-dependent partitioning between reservoirs determined self-consistently via climate with a given H_2 inventory (§3). As the atmospheric H_2 inventory is depleted via escape, the greenhouse effect also diminishes, accentuating the temperature-dependent partitioning between ocean and atmosphere. Hence, deuterium is further concentrated into the oceans due to the cooling

[1] The exchange reaction is $H_2O+HD \Leftrightarrow HDO+H_2$ with equilibrium constant $K(T)=1+0.22*(10^3/T)^2$.

426 radiative balance accompanying H_2 loss. In this way, D/H evolution of the oceans can be
427 calculated as an equilibrium distillation sequence, converging to a value determined by
428 the initial inventory of atmospheric H_2 (Fig. 5). Water molecules have a strong tendency
429 to concentrate deuterium, and, to the extent that hydrogen in other forms (e.g. H_2) are
430 significant species in the primordial atmosphere, highly pronounced D/H enrichments
431 (~2x) can arise from processing in this epoch, an enrichment not evident in the isotopic
432 record of Earth (see §5). Such enrichment can be minimized for a very oxidizing (H_2-
433 poor) atmospheres outgassed from the magma ocean. The D/H composition of the water
434 oceans immediately following primordial atmosphere evolution thereby constrains the
435 H_2/H_2O ratio of Earth's outgassed atmosphere to <0.3 and logfO_2 of last equilibration to
436 >IW+1. For a given H_2O abundance, e.g., 1-2 modern ocean equivalents (Korenaga,
437 2008), upper limits on the initial atmospheric H_2 inventory of Earth (pH_2<10-20 bars)
438 can be derived (Fig. 5).

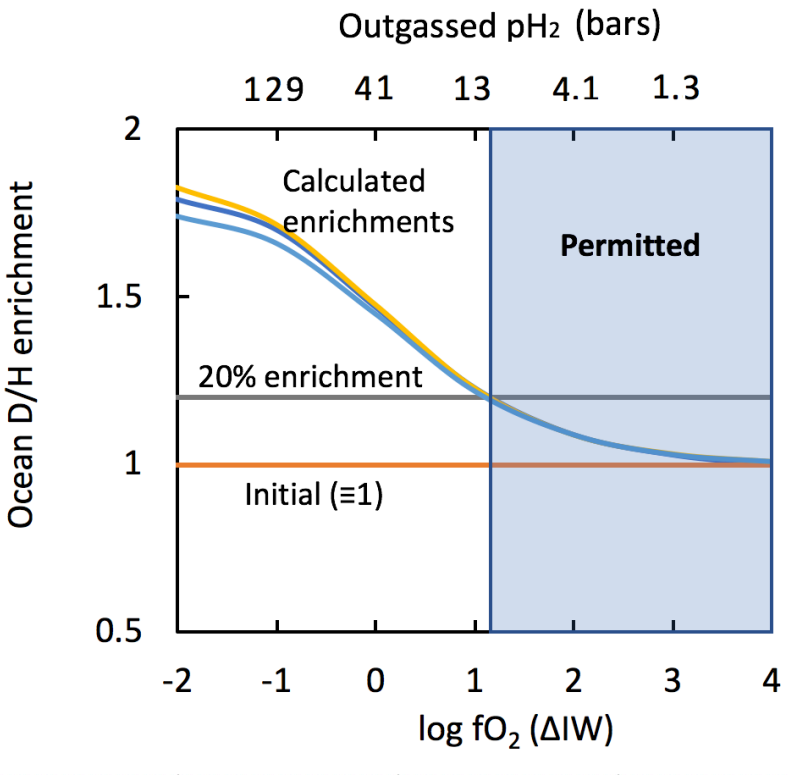

Figure 5 – Ocean deuterium enrichment versus oxygen fugacity of primordial outgassing. Oxygen fugacity determines the H_2/H_2O of the outgassed atmosphere. Oxidizing conditions ($\log fO_2$~IW+4≈QFM) lead to nearly "pure" steam atmospheres (H_2/H_2O<0.01, see Fig. 2) and minimal D-enrichment in the oceans. More reducing conditions for outgassing (e.g. $\log fO_2$<IW) generate higher H_2/H_2O values (>1) and stronger ocean deuterium enrichments (>1.5-2x) due to equilibrium partitioning and loss of large quantities of isotopically light H_2. Minimal (<20%) D-enrichment in terrestrial water relative to the source (§5) constrains the H_2/H_2O of the primordial atmosphere to <0.3 and therefore $\log fO_2$ of outgassing to >IW+1 (Permitted region). H_2 abundances can be expressed in absolute terms (top axis) by fixing water abundances to the terrestrial ocean reservoir (pH_2O=270 bars). Temperatures of equilibration are calculated via the climate model (§3), with enrichment curves representing different emission temperatures (T_e=215, 235, 255K) demonstrating the robustness of the result.

439 Here, we have only considered ocean-atmosphere partitioning followed by the escape of
440 atmospheric H_2 with no isotopic fractionation during the escape process. Consideration
441 of kinetic processes (e.g. HD/H_2 mass-fractionation) will fractionate H isotopes further
442 (Zahnle et al., 1990) and cause additional oceanic deuterium enrichment for a given H_2
443 inventory (Genda and Ikoma, 2008). The constraints on primordial H_2 abundances shown
444 in Figure 5 are, therefore, conservative upper limits.
445
446 **5. Discussion**
447 The molecular composition of the Earth's primordial atmosphere is not well-constrained.
448 Nevertheless, on the basis of their isotopic compositions, the Earth's major volatiles (H,
449 N, C) are thought to be sourced primarily from the carbonaceous chondrites (Alexander
450 et al., 2012; Halliday, 2013; Marty, 2012). This widely-held view of the source of major
451 terrestrial volatiles requires preservation of the source signature in the terrestrial oceans
452 and implies minimal D-enrichment via equilibration and escape of primordial H_2. To
453 quantify the constraint that this comparison places on primordial outgassing, we compare
454 the isotopic composition (δD=-25 +/- 5‰) of the Archean oceans (Pope et al., 2012) with
455 the lowest bulk chondritic values (δD=-226 +/- 4‰) measured to date (Alexander et al.,
456 2012). On this basis, a primarily chondritic source for terrestrial water requires minimal
457 (<20%) deuterium-enrichment via H_2 loss. According to our model calculations, this
458 level of isotopic preservation requires most outgassed hydrogen from the terrestrial
459 magma ocean to appear in the form of water vapor (H_2/H_2O<0.3, Fig. 5) and requires the
460 last equilibration with the magma ocean to be characterized by logfO_2 higher than IW+1.
461 By connecting the conditions of outgassing to the observable isotopic signatures of
462 ancient seawater, we can articulate new constraints on the composition of the Earth's

primordial atmosphere. These results show that reducing gases such as H_2 and CH_4 made up only a minor fraction of the Earth's outgassed atmosphere and require that the late-stage magma ocean was already oxidized by the time of last equilibration with the atmosphere. In this section, we discuss the implications of these results for redox evolution of the magma ocean (§5.1) and the oxidant involved in terrestrial late accretion (§5.2).

5.1. The redox state of the terrestrial magma ocean

The redox state of a magma ocean determines both the chemical composition of the outgassed atmosphere and the isotopic composition of the water ocean following primordial H_2 loss. Oxidizing magma oceans outgas water-rich primordial atmospheres, which condense into oceans, experiencing minimal hydrogen escape and deuterium enrichment. Reducing magma oceans, by contrast, outgas substantial quantities of hydrogen in non-condensable form (e.g. H_2) in addition to water molecules whose equilibration with the early water oceans can strongly (~2x) enrich water oceans in D/H, a feature not evident in the isotopic record of Earth (Pope et al., 2012). The persistence of a "chondritic" signature in the terrestrial oceans requires a low atmospheric H_2/H_2O at the time of last equilibration with a magma ocean, a ratio that acts as an oxybarometer, implying relatively oxidizing conditions ($\log fO_2 > IW+1$) for primordial outgassing. Given that the vigorously convective magma ocean initially held metallic droplets in suspension (Stevenson, 1990) and was therefore more chemically reducing ($\log fO_2 < IW-2$) at early times, these results suggest that the silicate Earth was oxidized *during* the evolution of the magma ocean. Three mechanisms have been discussed for this primordial oxidation: (1) the terrestrial magma ocean could have been oxidized via Fe disproportionation at high pressure ($3Fe^{+2} \rightarrow 2Fe^{+3} + Fe^0$) with separation of the newly

488 generated metallic iron to the core leaving an oxidized mantle residue (Wade and Wood,
489 2005), (2) the primordial atmosphere was reducing (H_2-rich) but the process of H_2 escape
490 during the lifetime of the magma ocean oxidized both silicate Earth and co-existing
491 atmosphere (Hamano et al., 2013), and (3) the (Fe^{+3}/Fe^{+2}) value of the terrestrial magma
492 ocean was low (~0.01) but the more incompatible nature of ferric iron (Fe^{+3}) in mantle
493 minerals enriched it in evolving liquids such that the late-stage magma was more
494 oxidizing than the magma ocean at the outset of crystallization (Schaefer et al. in prep).
495 The relative importance of these three processes for the redox evolution of magma oceans
496 is subject to future study. For now, we conclude that the oxidation of the silicate Earth
497 occurred during the crystallization of the magma ocean, independently corroborating the
498 conclusion from geological data for early (>4 Gya) establishment of oxidizing conditions
499 in the silicate Earth (Trail et al., 2011).
500
501 5.2. The oxidant for terrestrial late accretion
502 Before outgassing of the primordial atmosphere, the magma ocean potentially facilitates
503 the last major episode of core formation via separation of metallic droplets accompanying
504 deep magma ocean convection on rapid (~10^2 year) timescales (Stevenson, 1990). Such
505 metallic droplets strongly concentrate and efficiently scavenge highly siderophile
506 elements (HSEs) from the terrestrial magma ocean and sequester them into the metallic
507 core. Mantle relative abundances of HSEs resemble the chondrites, leading to the notion
508 that these elements were delivered during the final ~1% of Earth accretion, after cessation
509 of core formation (Kimura et al., 1974), now interpreted as accretion after the Moon-
510 forming giant impact. Isotopic characteristics of the Earth's mantle suggest delivery by
511 bodies with metallic phases either as undifferentiated metallic grains or as planetesimal
512 cores (Marchi et al., 2018). However, the terrestrial upper mantle is currently unsaturated

513 in metallic Fe, instead exhibiting a more oxidizing redox state, indicated by higher
514 Fe^{+3}/Fe^{+2} values than those characterizing co-existence with metallic iron. Accordingly,
515 accreted metals must have been oxidized and dissolved into Earth's mantle, prompting
516 the question of the nature of the oxidant involved in late accretion. Since the terrestrial
517 magma ocean crystallized on ~10^6 year timescales (Lebrun et al., 2013) while the
518 leftovers of terrestrial planet accretion were swept up over ~10^7-10^8 years (Morbidelli et
519 al., 2012), late accretion occurred onto a solid silicate Earth with well-developed water
520 oceans. Possibilities for oxidizing metals delivered during late accretion are: (1) Earth's
521 fluid envelope, e.g. water in the terrestrial oceans, via the iron-water reaction
522 ($Fe+H_2O \rightarrow FeO+H_2$) followed by hydrodynamic escape of H_2 (Genda et al., 2017) and
523 (2) the oxidizing power of Earth's mantle, epitomized by ferric iron ($2Fe^{+3}+Fe^0 \rightarrow 3Fe^{+2}$),
524 lowering the ferric iron abundance towards the modern upper mantle value
525 (Fe^{+3}/Fe^{+2}=0.03-0.04) (Canil et al., 1994). Using calculated enrichments in the D/H of
526 water oceans coexisting with significant (~10-100 bar) early H_2 atmospheric inventories,
527 we can limit the extent of the iron-water reaction in oxidizing the metals of late accretion.
528 Given that the oxidation of metals at that time would consume more than a modern ocean
529 worth of water via the iron-water reaction (producing >30 bars H_2) and that the Hadean
530 H_2 inventory was apparently <10-20 bars (Fig. 5), we conclude that the role of the iron-
531 water reaction during late accretion was subdominant. A more dominant role for this
532 reaction would have produced deuterium-enriched oceans not observed in the terrestrial
533 isotopic record. This reasoning suggests that the terrestrial mantle supplied oxidants
534 during late accretion, a feature that may yield insights into the physics and chemistry of
535 this early terrestrial process.
536
537 **6. Conclusions**

538 The isotopic composition of the oceans provides a unique constraint for early planetary
539 evolution. It is widely accepted that most water accreted by the Earth was delivered
540 before the Moon-forming giant impact and that most water dissolved in the subsequent
541 magma ocean was excluded from crystallizing minerals and outgassed into the
542 primordial atmosphere (Elkins-Tanton, 2008; Greenwood et al., 2018). Given that the
543 residence time of water in the Earth's oceans is comparable to, or greater than, the current
544 age of the Earth (van Keken et al., 2011), most of the hydrogen in the oceans today is
545 inferred to be outgassed from the magma ocean, retaining isotopic memory of the
546 chemical composition of the primordial atmosphere.
547
548 The oxygen fugacity of terrestrial magma ocean outgassing – and therefore the chemical
549 composition of the primordial atmosphere – has not been independently constrained. By
550 linking the oxygen fugacity of primordial outgassing to the deuterium content of Earth's
551 hydrosphere, we articulate new constraints on these critical parameters governing early
552 Earth evolution. We find that preservation of a carbonaceous chondritic D/H signature
553 in the terrestrial oceans (to ~10-20%) requires the primordial terrestrial fluid envelope
554 be hydrogen-poor ($H_2/H_2O<0.3$), indicating oxidizing conditions ($\log fO_2>IW+1$) for last
555 equilibration with the magma ocean. We infer that oxidation of the silicate Earth took
556 place during the evolution of Earth's final magma ocean, and may require no geological
557 oxidation processes (e.g. subduction) to be consistent with an oxidized mantle (Trail et
558 al., 2011) observed in the earliest terrestrial record.
559
560 The inferred absence of massive (>20 bar) H_2 inventories of any origin on the Hadean
561 Earth constrains the oxidant for terrestrial late accretion. Whereas the likely existence of
562 early water oceans has previously been taken to imply that the iron-water reaction was

563 responsible for oxidizing the metals delivering HSEs to the early Earth (Genda et al.,
564 2017), we find that such massive reduction would have disturbed the carbonaceous-
565 chondrite-like signature of the terrestrial oceans. We therefore infer that oxidants in the
566 terrestrial mantle (e.g. Fe^{+3}) were responsible for oxidative resorption of late-accreting
567 metals delivered to the Earth. Indeed, the oxidative potential of Earth's modern mantle
568 (Canil et al., 1994) is comparable to the reducing potential in ~0.5% of an Earth mass of
569 chondritic late accretion, a feature that may yield insight into this early process.
570
571 **Acknowledgements**
572 K.P. acknowledges support from a grant from the W.M. Keck foundation (PI: Peter
573 Buseck).
574
575 **References**

576 Abe, Y., Matsui, T., 1988. Evolution of an impact-generated H2O–CO2 atmosphere
577 and formation of a hot proto-ocean on Earth. Journal of the Atmospheric Sciences
578 45, 3081-3101.
579 Alexander, C.O.D., Bowden, R., Fogel, M., Howard, K., Herd, C., Nittler, L., 2012. The
580 provenances of asteroids, and their contributions to the volatile inventories of the
581 terrestrial planets. Science 337, 721-723.
582 Archer, D., Eby, M., Brovkin, V., Ridgwell, A., Cao, L., Mikolajewicz, U., Caldeira, K.,
583 Matsumoto, K., Munhoven, G., Montenegro, A., Tokos, K., 2009. Atmospheric
584 Lifetime of Fossil Fuel Carbon Dioxide. Annual Review of Earth and Planetary
585 Sciences 37, 117-134.
586 Brown, H., 1949. Rare gases and the formation of the Earth's atmosphere, The
587 Atmospheres of the Earth and Planets, p. 258.
588 Canil, D., O'Neill, H.S.C., Pearson, D., Rudnick, R., McDonough, W., Carswell, D., 1994.
589 Ferric iron in peridotites and mantle oxidation states. Earth and Planetary Science
590 Letters 123, 205-220.
591 Chase, M.W., Davies, C.A., Downey, J.R., Frurip, D.J., Mcdonald, R.A., Syverud, A.N.,
592 1985. Janaf Thermochemical Tables - 3rd Edition .2. Journal of Physical and
593 Chemical Reference Data 14, 927-1856.
594 Delano, J.W., 2001. Redox history of the Earth's interior since~ 3900 Ma:
595 implications for prebiotic molecules. Origins of Life and Evolution of the Biosphere
596 31, 311-341.
597 Elkins-Tanton, L.T., 2008. Linked magma ocean solidification and atmospheric
598 growth for Earth and Mars. Earth and Planetary Science Letters 271, 181-191.

599 Elkins-Tanton, L.T., 2012. Magma Oceans in the Inner Solar System. Annual Review
600 of Earth and Planetary Sciences 40, 113-139.
601 Erkaev, N., Lammer, H., Odert, P., Kislyakova, K., Johnstone, C., Güdel, M.,
602 Khodachenko, M., 2016. EUV-driven mass-loss of protoplanetary cores with
603 hydrogen-dominated atmospheres: the influences of ionization and orbital
604 distance. Monthly Notices of the Royal Astronomical Society 460, 1300-1309.
605 Frost, B.R., 1991. Introduction to oxygen fugacity and its petrologic importance.
606 Reviews in Mineralogy and Geochemistry 25, 1-9.
607 Genda, H., Brasser, R., Mojzsis, S.J., 2017. The terrestrial late veneer from core
608 disruption of a lunar-sized impactor. Earth and Planetary Science Letters 480, 25-
609 32.
610 Genda, H., Ikoma, M., 2008. Origin of the ocean on the Earth: Early evolution of water
611 D/H in a hydrogen-rich atmosphere. Icarus 194, 42-52.
612 Gough, D., 1981. Solar interior structure and luminosity variations. Solar Physics 74,
613 21-34.
614 Greenwood, R.C., Barrat, J.-A., Miller, M.F., Anand, M., Dauphas, N., Franchi, I.A.,
615 Sillard, P., Starkey, N.A., 2018. Oxygen isotopic evidence for accretion of Earth's
616 water before a high-energy Moon-forming giant impact. Science Advances 4.
617 Halliday, A.N., 2013. The origins of volatiles in the terrestrial planets. Geochimica Et
618 Cosmochimica Acta 105, 146-171.
619 Hamano, K., Abe, Y., Genda, H., 2013. Emergence of two types of terrestrial planet
620 on solidification of magma ocean. Nature 497, 607-610.
621 Hirschmann, M.M., 2012. Magma ocean influence on early atmosphere mass and
622 composition. Earth and Planetary Science Letters 341–344, 48-57.
623 Hunten, D., 1973. The Escape of Light Gases from Planetary Atmospheres. Journal
624 of the Atmospheric Sciences 30, 1481-1494.
625 Ikoma, M., Elkins-Tanton, L., Hamano, K., Suckale, J., 2018. Water Partitioning in
626 Planetary Embryos and Protoplanets with Magma Oceans. Space Science Reviews
627 214, 76.
628 Ingersoll, A.P., 1969. The Runaway Greenhouse: A History of Water on Venus.
629 Journal of the Atmospheric Sciences 26, 1191-1198.
630 Kasting, J.F., 1988. Runaway and moist greenhouse atmospheres and the evolution
631 of Earth and Venus. Icarus 74, 472-494.
632 Kasting, J.F., 2014. Atmospheric composition of Hadean–early Archean Earth: The
633 importance of CO, in: Shaw, G.H. (Ed.), Earth's Early Atmosphere and Surface
634 Environment. Geological Society of America.
635 Kimura, K., Lewis, R.S., Anders, E., 1974. Distribution of gold and rhenium between
636 nickel-iron and silicate melts: implications for the abundance of siderophile
637 elements on the Earth and Moon. Geochimica et Cosmochimica Acta 38, 683-701.
638 Korenaga, J., 2008. Plate tectonics, flood basalts and the evolution of Earth's oceans.
639 Terra Nova 20, 419-439.
640 Kurokawa, H., Foriel, J., Laneuville, M., Houser, C., Usui, T., 2018. Subduction and
641 atmospheric escape of Earth's seawater constrained by hydrogen isotopes. Earth
642 and Planetary Science Letters 497, 149-160.
643 Lebrun, T., Massol, H., Chassefière, E., Davaille, A., Marcq, E., Sarda, P., Leblanc, F.,
644 Brandeis, G., 2013. Thermal evolution of an early magma ocean in interaction with
645 the atmosphere. Journal of Geophysical Research: Planets 118, 1155-1176.
646 Lécluse, C., Robert, F., 1994. Hydrogen isotope exchange reaction rates: Origin of
647 water in the inner solar system. Geochimica et Cosmochimica Acta 58, 2927-2939.

Lécuyer, C., Gillet, P., Robert, F., 1998. The hydrogen isotope composition of seawater and the global water cycle. Chemical Geology 145, 249-261.
Lesher, C.E., Spera, F.J., 2015. Thermodynamic and transport properties of silicate melts and magma, The Encyclopedia of Volcanoes (Second Edition). Elsevier, pp. 113-141.
Marchi, S., Canup, R., Walker, R., 2018. Heterogeneous delivery of silicate and metal to the Earth by large planetesimals. Nature Geoscience 11, 77.
Marty, B., 2012. The origins and concentrations of water, carbon, nitrogen and noble gases on Earth. Earth and Planetary Science Letters 313, 56-66.
Morbidelli, A., Marchi, S., Bottke, W.F., Kring, D.A., 2012. A sawtooth-like timeline for the first billion years of lunar bombardment. Earth and Planetary Science Letters 355, 144-151.
Pahlevan, K., Morbidelli, A., 2015. Collisionless encounters and the origin of the lunar inclination. Nature 527, 492-494.
Pierrehumbert, R.T., 2010. Principles of planetary climate. Cambridge University Press.
Pope, E.C., Bird, D.K., Rosing, M.T., 2012. Isotope composition and volume of Earth's early oceans. Proceedings of the National Academy of Sciences 109, 4371-4376.
Ribas, I., Guinan, E.F., Güdel, M., Audard, M., 2005. Evolution of the solar activity over time and effects on planetary atmospheres. I. High-energy irradiances (1-1700 Å). The Astrophysical Journal 622, 680.
Richet, P., Bottinga, Y., Javoy, M., 1977. Review of Hydrogen, Carbon, Nitrogen, Oxygen, Sulfur, and Chlorine Stable Isotope Fractionation among Gaseous Molecules. Annual Review of Earth and Planetary Sciences 5, 65-110.
Schaefer, L., Fegley, B., 2010. Chemistry of atmospheres formed during accretion of the Earth and other terrestrial planets. Icarus 208, 438-448.
Stevenson, D.J., 1990. Fluid Dynamics of Core Formation, Origin of the Earth, pp. 231-249.
Trail, D., Watson, E.B., Tailby, N.D., 2011. The oxidation state of Hadean magmas and implications for early Earth's atmosphere. Nature 480, 79.
van Keken, P.E., Hacker, B.R., Syracuse, E.M., Abers, G.A., 2011. Subduction factory: 4. Depth ‐ dependent flux of H2O from subducting slabs worldwide. Journal of Geophysical Research: Solid Earth 116.
Wade, J., Wood, B.J., 2005. Core formation and the oxidation state of the Earth. Earth and Planetary Science Letters 236, 78-95.
Watson, A.J., Donahue, T.M., Walker, J.C.G., 1981. The dynamics of a rapidly escaping atmosphere: Applications to the evolution of Earth and Venus. Icarus 48, 150-166.
Wordsworth, R., 2012. Transient conditions for biogenesis on low-mass exoplanets with escaping hydrogen atmospheres. Icarus 219, 267-273.
Wordsworth, R., Pierrehumbert, R., 2013a. Hydrogen-Nitrogen Greenhouse Warming in Earth's Early Atmosphere. Science 339, 64-67.
Wordsworth, R.D., Pierrehumbert, R.T., 2013b. Water loss from terrestrial planets with CO2-rich atmospheres. The Astrophysical Journal 778, 154.
Zahnle, K., Kasting, J.F., Pollack, J.B., 1990. Mass fractionation of noble gases in diffusion-limited hydrodynamic hydrogen escape. Icarus 84, 502-527.
Zhang, Y., Xu, Z., Zhu, M., Wang, H., 2007. Silicate melt properties and volcanic eruptions. Reviews of Geophysics 45, n/a-n/a.